

LABORATORY OBSERVATIONS OF DISSOLVED CARBON DIOXIDE TRANSPORT UNDER REGULAR BREAKING WAVES

Junichi Otsuka, Civil Engineering Research Institute for Cold Region, 08900@ceri.go.jp
 Yasunori Watanabe, Hokkaido University, yasunori@eng.hokudai.ac.jp

INTRODUCTION

Air bubbles and strong turbulence that form in water from breaking waves play important roles in gas transfer across the air-sea interface (Melville, 1996). The entrained bubbles increase the total area of air-water interface per unit volume and enhance local gas dissolution into water. The dissolved gases mix in the water mass diffuse by the strong turbulence. These gas transfer-enhancing factors have been parameterized by only wind speed in models of gas transfer velocity in the deep ocean. Bulk parameters based on wind speed cannot be used for a surf zone, where waves break due to shoaling. In a surf zone, the cross-shore distributions of entrained bubbles and the turbulent intensity vary as waves propagate. The physical process of gas transfer under the complex air-water turbulent flows in breaking waves has not been clarified. Thus, breaking-wave factors that enhance gas transfer in a surf zone cannot be parameterized.

In this study, we observed the transport process of dissolved carbon dioxide (DCO₂) under air-water turbulent flows in a laboratory surf zone using image measurement systems.

EXPERIMENTS

Experiments were conducted in a wave flume of 8.1 m in length, 0.3 m in width and 0.6 m in depth equipped with a 1/20.8 sloping bottom. The walls, bottom and cover of the flume were made of transparent acrylic. CO₂ was supplied to the gas phase over the wave interface from a compressed CO₂ cylinder. DCO₂ concentration, fluid velocity and entrained air bubbles in the surf zone were measured using laser-induced fluorescence (LIF), particle image velocimetry (PIV) and LED backlight, respectively. These image measurements were made at the same cross-shore locations that were traversed at 20-cm intervals from the wave breaking point to the shoreline using a high-speed video camera (8-bit, 250 fps, 1000×1000 pixels, 20×20-cm field of view). In the experiments, regular waves with a period of 1.5 s, a breaking wave depth of 13.9 cm, a breaking wave height of 13.0 cm were generated. The waves broke as spilling-plunging breakers.

RESULTS

In the surf zone, plunging jets of breaking waves sequentially splashed onto the leading water surface, producing strong turbulence in the transition region (Fig 1, $x = 50 - 140$ cm), which lead to a fully developed turbulent bore in the bore region (Fig 1, $x = 140 - 240$ cm).

In the transition region, a large number of air bubbles were produced in the water (Fig 1 (d), $x = 50 - 140$ cm). The entrained bubbles were trapped within obliquely descending eddies and were transported toward the bottom. In the transport process, we observed from the LIF measurements that CO₂ was supplied from each bubble to the water. Although local gas supply from the bubbles was active in the transition region, the spatial concentration of DCO₂ did not easily increase (Fig 2, $x = 50 - 140$ cm) because the local dissolved gas from the

bubbles was mixed in the deep water mass by strong turbulence.

In the bore region, there are far fewer entrained bubbles than in the transition region (Fig 1 (d), $x = 140 - 240$ cm). Although CO₂ was supplied to the water by the few bubbles, the DCO₂ concentration spatially increased and reached a high level in a short time (Fig 2, $x = 140 - 240$ cm) because the water was shallow.

In the surf zone, undertow typically developed under the wave trough level (Fig 1 (a)). It seems that the undertow transported the concentrated DCO₂ in the bore region toward the wave breaking point through locations near the bottom, where lower turbulence was produced. Therefore, to model the gas transfer velocity in a surf zone, we need to parameterize the breaking-wave factors, such as entrained bubbles and turbulent intensity, that are associated with the undertow.

REFERENCE

Melville (1996): The role of surface-wave breaking in air-sea interaction, *Ann Rev of Fluid Mech*, 28, pp. 279-321.

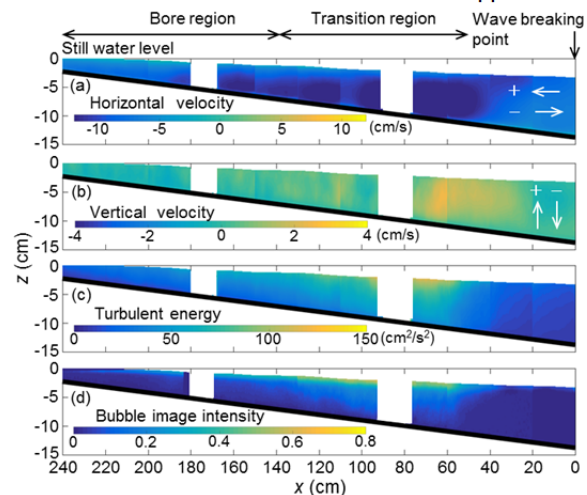


Figure 1 Cross-shore distributions of time-averaged (a) horizontal velocity, (b) vertical velocity, (c) turbulent energy and (d) bubble image intensity (x : distance from the wave-breaking point, z : distance from the still-water level)

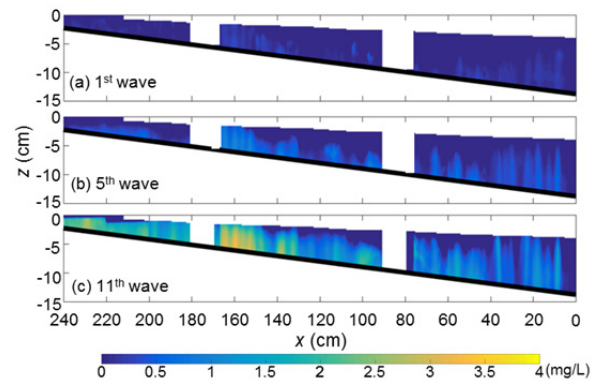


Figure 2 Cross-shore distributions of time-averaged DCO₂ concentration